1 January 1999

ELSEVIER

Chemical Physics Letters 299 (1999) 25–34

CHEMICAL PHYSICS LETTERS

Quasiclassical trajectory study of the Li + HF($v = 0$) → LiF + H reaction

F.J. Aoiz [a], M.T. Martínez [b], M. Menéndez [a], V. Sáez Rábanos [c], E. Verdasco [a,*]

[a] *Departamento de Química Física, Facultad de Química, Universidad Complutense, 28040 Madrid, Spain*

[b] *Departamento de Máquinas y Motores Térmicos, EU de Ingenieros Técnicos Industriales, Universidad del País Vasco, 48012 Vizcaya, Spain*

[c] *Departamento de Química General y Bioquímica, ETS Ingenieros de Montes, Universidad Politécnica, 28040 Madrid, Spain*

Received 24 June 1998; in final form 16 October 1998

Abstract

Quasi-classical trajectory (QCT) calculations for the Li + HF($v = 0$, j) → LiF + H reaction have been performed on a recent ab initio potential energy surface (PES). Integral and differential cross-sections, as well as angle–velocity polar maps, have been calculated at the collision energies and initial rotational states of HF($v = 0$, $j = 0$–3) relevant to the experiment of Becker et al. (J. Chem. Phys. 73 (1980) 2833). With these theoretical results, the laboratory angular distributions (LAB-AD) have been simulated and compared with experiment. The main features of the experimental LAB-AD and energy-dependent cross-section are qualitatively reproduced. In addition, the QCT total reaction cross-section as a function of the collision energy is compared with an approximate quantum mechanical calculation on the same PES.

1. Introduction

Since the early 1980s, a great deal of experimental [1–4] and theoretical [5–31] work has been devoted to the Li + HF reaction as a prototype of a heavy–heavy–light (**HHL**) system, becoming a benchmark in molecular reaction dynamics. This reaction is known to have a strongly bent transition state, and this feature is expected to add a considerable richness to its dynamics.

From the experimental point of view, the reaction has been studied by Becker et al. [1] in a crossed molecular beam experiment, detecting the LiF product by mass spectrometry. Product laboratory angular distributions (LAB-AD) and time-of-flight (TOF) spectra were measured at several collision energies ranging from 95 to 377 meV (2.2–8.7 kcal mol^{-1}). The analysis of the results yielded center-of-mass (CM) triple scattering angle-recoil velocity differential cross-sections (DCS) at two collision energies (130 and 377 meV), as well as the collision energy (E_T) dependence of the total reaction cross-section, $\sigma_R(E_T)$.

More recently Loesch and coworkers [2–4] have reported a detailed crossed molecular beam study on the Li + HF($v = 1$, $j = 1$, $m = 0$) reaction at the collision energy $E_T = 420$ meV. The reaction was studied for three different distributions of the HF internuclear axis, and pronounced steric effects were found in the integral cross-section and in the products angular and recoil velocity distributions. The analy-

* Corresponding author. Fax: +34 91 394 4135; e-mail: quique@orion.quim.ucm.es

0009-2614/99/$ - see front matter
PII: S0009-2614(98)01247-0

sis of these data rendered three moments of the orientation-dependent DCS, which indicate a preference for the broad side attack.

The relative simplicity of the system makes it attractive for theoretical treatments, and, as such, there exists a long saga of theoretical calculations, the number of which is growing rapidly, especially in the last few years. There are already a series of semi-empirical [5–7] and ab initio potential energy calculations [8–11]. Chen and Schaefer [9] carried out a SCF-CISD (single configuration) set of ab initio calculations at different geometries, but the resulting height of the barrier at the transition state was found to be too large (434 meV, 10 kcal mol^{-1}) for a realistic description of the reaction. To overcome this problem, Carter and Murrell produced a fit [13] reducing the barrier to 170 meV. Laganà and coworkers have produced several PES fits after suitable semi-empirical adjustments of the ab initio points of Chen and Schaefer [14,16]. In particular, Palmieri and Laganà [15] carried out some ab initio calculations at some critical points, resulting in a lowering of the barrier to reaction. The latest global fit [16] (hereafter Laganà PES), produced by scaling the original ab initio results of Chen and Schaefer, gives a bent transition state (Li–F–H angle 74°) located in the exit channel, with a barrier of 182 meV. More recently, Paniagua and coworkers have performed MRDCI calculations of the ground and lower excited states PESs of the LiFH system [11,12], and subsequently fitted the ab initio points [17] to study the dynamics of the ground state reaction. They found that the barrier to the reaction at an angle of 73° was 249 meV (233 meV in the latest global fit of the PES [32], see below) above the minimum of the reactants, somewhat larger than the value of the Laganà PES.

The availability of, in principle, reliable PESs has prompted numerous dynamical calculations using the quasi-classical trajectory (QCT) approach [4,18, 21,25,29] or, more recently, time-independent [16,23,24,27–29] and time-dependent [30,31] quantum mechanical (QM) methods aimed at reproducing the existing experimental results. Laganà and coworkers [19,21,29] have extensively explored this reaction using the QCT approach on a variety of PESs. Loesch and Stienkemeier [4] also carried out QCT calculations for the $Li + HF(v = 1)$ reaction and for different distributions of the HF internuclear axis on a modified version of the Carter and Murrell fit of the Chen and Schaefer PES. The QCT results were in qualitative agreement with the experimentally deduced differential cross-sections and proved to be useful for their interpretation.

Due to the complications inherent in accurate full-dimensional QM calculations, most of the QM results are restricted to the reaction with zero total angular momentum, using various approximations to calculate reaction probabilities for $J \neq 0$. However, the rapid progress which the field is experiencing permits us to foresee that fully converged accurate QM calculations for all partial waves needed to evaluate reaction cross-sections will be soon available.

Accurate quantum reactive probabilities for zero total angular momentum have been reported by Parker et al. [16] on the Laganà PES using hyperspherical coordinates. Narrow and broad resonances were related to quantum interferences between states connecting reactants and products and were analyzed in terms of the energy levels of the bound states supported by the wells of the effective potential curves. Gögtas et al. [30] used the time-dependent approach to calculate reaction probabilities at $J = 0$ on the same PES. As in the calculations of Parker et al., the scattering at low energies is dominated by sharp resonance features. More recently, Zhu et al. [31] carried out time-dependent calculations for collision energies up to 400 meV also on the Laganà PES. Accurate reaction probabilities for $J = 0$ were computed and, using the centrifugal sudden (CS) approximation, the reaction cross-section was evaluated. It was found that, whereas at low collision energies the reaction proceeds mainly by an indirect mechanism involving long-lived resonances, at higher collision energies the direct reaction becomes more important, with an almost total disappearance of the resonance structure in the reaction probability.

Aguado et al. [17] have carried out wavepacket calculations on their original PES, and they found a substantially lower reactivity than on the Laganà PES. Subsequently, a new more-refined fit, using many more ab initio points, has been produced by the same authors [32] (hereafter AP2–PES), resulting in a lowering of the saddle-point energy to 0.233 eV and the suppression of spurious features of the initial fit. Wavepacket calculations on their new fit yielded

larger reaction probabilities at $J = 0$, and larger CS cross-sections [32], similar in absolute value to those calculated by Zhu et al. [31] on the Laganà PES at high collision energies, but with a different behaviour at energies below 250 meV.

The availability of this latest global fit for a large number of ab initio points provides a good opportunity for the simulation of the experiments of Becker et al. [1]. In this Letter, QCT calculations have been carried out on the AP2–PES in order to compare with the results of the above-mentioned experiments and, in the case of the excitation functions, with the corresponding QM results. Calculations have been also performed on the widely used Laganà PES [16] to compare with the results obtained on the AP2–PES.

2. QCT method and theoretical simulations

The general methodology of the QCT calculation is the same as used in previous works. It is described more extensively in Ref. [33], and only the particular details relevant to the present work will be given here.

Calculations on the ab initio AP2–PES [32] have been performed for the Li + HF($v = 0$, $j = 0$–3) reaction at 130 meV (3.0 kcal mol^{-1}) and 377 meV (8.7 kcal mol^{-1}) collision energies corresponding to the two mean collision energies of the molecular beam experiment of Becker et al. [1], for which LAB-AD and TOF spectra were reported. Batches ranging from 30000 to 60000 trajectories have been calculated at each energy and initial rotational quantum number j. Since the potential has long-range forces in both the entrance and exit channels, the trajectories were started and finished at a distance from the atom to the CM of the diatom of 12 Å. At low collision energies, these distances imply integrations times up to 25 ps. The value of the maximum impact parameter, b_{max}, used in the calculations ranged from 1.8 to 3.4 Å, depending on E_T and j. To calculate the collision energy dependence of the total reactive cross-section, $\sigma_R(E_T)$, for initial $j = 0$, a batch of 2×10^5 trajectories was run by randomly varying the collision energy in each trajectory in the interval from 25 to 500 meV. The $\sigma_R(E_T)$ is subsequently calculated by the method of moment expansion in Legendre polynomials, as described in detail in Ref. [34]. To check the reliability of this procedure for this reaction, batches of 10^4 to 3×10^4 trajectories were run at a series of fixed collision energies and $j = 0$.

In addition, batches of 6×10^4 and 3×10^4 trajectories have been calculated for the title reaction at 130 and 377 meV collision energies, respectively, and initial $j = 0$–3, on the latest PES of the series produced by Laganà and coworkers [16] (Laganà PES) to compare with the results on the AP2–PES. Values of b_{max} in this PES were also similar to the ones used in AP2–PES. Additional batches of $\approx 10^4$ trajectories were run at several other collision energies and $j = 0$–3 to determine the excitation function on this PES. In total, the number of trajectories relevant to this work is ca. 1.0×10^6.

The rovibrational initial energies of HF and LiF were calculated by semiclassical quantization of the classical action, using in each case the asymptotic diatomic potential of the corresponding PES (see Ref. [33] and cites therein). For both reagent and product molecules, the quantization of the rotation is performed by equating the square of the rotational angular momentum to $j(j+1)\hbar^2$.

The reactive differential cross-sections $d\sigma_R/d\omega$ were calculated by the method of moments expansion in Legendre polynomials [33]. Significance levels higher than 99% could be achieved using 3–10 Legendre moments, ensuring a good convergence, such that the inclusion of more terms does not produce any significant change. The error bars, calculated as in Ref. [33], correspond to ± 1 standard deviation.

Similarly, the triple angle–velocity differential cross-sections $d\sigma_R/d\omega\, dw'$ were determined by fitting to a double series of Legendre polynomials with arguments $\cos\theta$ and the reduced recoil velocity r defined as $r = 2w'/w_{max} - 1$, where w' is the LiF recoil velocity and w_{max} is its maximum value given by the energy conservation. Angle–velocity contour polar maps are derived from this double expansion for each individual j, and then they were weighted with the experimental distribution of initial j states of HF molecules, so that:

$$\left\langle \frac{d\sigma_R}{d\omega\, dw'} \right\rangle = \sum_{j=0}^{3} P(j) \left[\frac{d\sigma_R}{d\omega\, dw'} \right]_j . \qquad (1)$$

In the original work by Becker et al. [1] the distribution of HF rotational states $P(j)$ was not measured. However, in latter experiments by the group of Loesch, the rotational distribution in HF molecular beams under similar expansion conditions was determined by laser-induced fluorescence infrared spectroscopy [35], and it could be characterized by a Boltzmann temperature of ≈ 86 K, which gives as relative populations for $j = 0–3$, 0.314, 0.465, 0.189 and 0.032, respectively. We have used these weights throughout this work.

Simulation of the LAB-AD of scattered LiF molecules is carried out by transforming the theoretical CM DCS into the LAB system. The signal at a LAB angle Θ can be expressed as:

$$S(\Theta) = \sum_j P(j) \int \mathrm{d}^3\,\mathbf{r}\, n_1(\mathbf{r}) n_2(\mathbf{r}) \int \mathrm{d}\Omega\, D(\Omega) \times \int\int \mathrm{d}v_1\, \mathrm{d}v_2\, f(v_1) f(v_2)\, v_\mathrm{r} \times \int \mathrm{d}v'\, \frac{2}{w'_{\max}} \left(\frac{\mathrm{d}\sigma}{\mathrm{d}\omega\, \mathrm{d}r} \right)_j \frac{v'}{w'^2}. \quad (2)$$

The procedure consists of a Monte Carlo sampling of the reagents' beam velocities $f(v_1)$, $f(v_2)$ and spatial beam densities $n_1(\mathbf{r})$, $n_2(\mathbf{r})$ where the position vector $\mathbf{r}$ refers to a point in the scattering volume defined by the beam divergences and the geometry of the experiment [1]. The signal at a given LAB angle is obtained by integration over the LAB velocity of the products v'. In this equation, the function $D(\Omega)$ accounts for the detector aperture in and out of the scattering plane, v_r is the relative velocity and the sum in j extends to all initial rotational quantum number j of the HF reagent. The v'/w'^2 factor accounts for the jacobian of the CM to LAB transformation when product density is detected. The simulated LAB-AD are scaled to the experimental ones by a least-squares procedure.

3. Results and discussion

The upper panel of Fig. 1 shows the total reaction cross-section calculated for the Li + HF($v = 0$, $j = 0$) on the AP2–PES in the collision energy range of 25–470 meV, as well as the corresponding excitation function calculated by Aguado et al. [32] using a time-dependent treatment and the centrifugal sudden (CS) approximation for $J > 0$. The QM $\sigma_\mathrm{R}(E_\mathrm{T})$ has a series of maxima but, on average, tends to increase with E_T. In contrast, the QCT cross-section has a sharp maximum at 75 meV, after which it increases slowly for E_T larger than 150 meV. At low collision energies the QM $\sigma_\mathrm{R}(E_\mathrm{T})$ is significantly smaller than the classical one. No neat threshold is found in any of the two calculations but, in the QM case, the value of the cross-section at the lowest energy calcu-

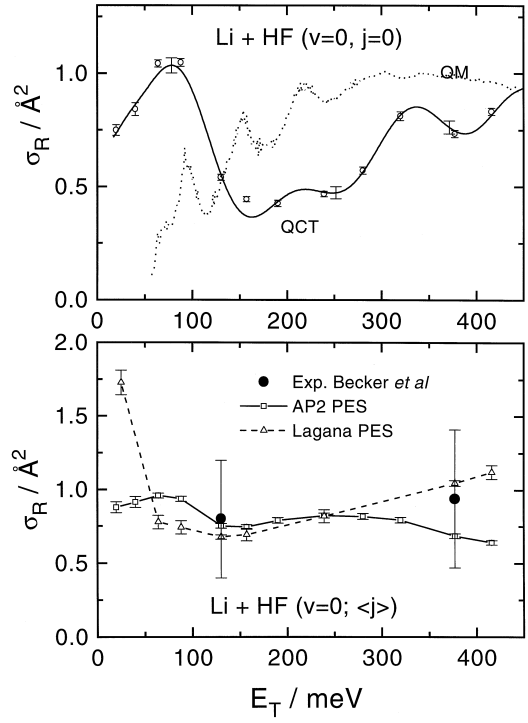

Fig. 1. Collision energy dependence of the total integral reaction cross-section (excitation function). (Top) Present QCT (solid line and circles) and QM (dotted line) from Ref. [17] for the Li + HF ($v = 0$, $j = 0$) reaction calculated on the AP2–PES. The solid line was calculated by running a batch of trajectories whose collision energy is randomly sampled between the interval 25–500 meV (see Section 2). The circles represent the QCT calculations carried out at fixed collision energies. (Bottom) Reaction cross-section averaged on the experimental initial rotational state distribution. Squares and solid line are QCT calculations on the AP2–PES. Triangles and dashed line are QCT calculations on the Laganà PES. Circles are experimental values from Ref. [1]; the experimental error bars represent the estimated uncertainty in the absolute values of the cross-section.

lated is much smaller than the classical one. Therefore, the QCT results are at variance with the QM calculations. A major difference between the QM and QCT approaches lies in the effect of the zero-point energy of the activated complex, which in the QCT case is neglected. From the $v = 0$ state of the HF molecule, the classical passage through the barrier is an exoergic process by ≈ 20 meV on the AP2–PES. However, by including the zero-point energy of the saddle point (322 meV above the minimum of the reagents [32]), the process is endoergic by 68 meV. Therefore, for energies below this value one can expect that only indirect reaction, through tunneling, might take place. The low value of the QM reactive cross-section at ≈ 50 meV seems to indicate that there is a threshold for this reaction or, at least, a substantially lower reactivity than the one obtained in the QCT calculations. The analysis of classical time delays clearly shows that at low collision energies most of the reaction occurs via long-lived trajectories, which can last up to several picoseconds, whereas those non-reactive trajectories can be either direct or non-direct, depending on whether they sample the reactive well. As the collision energy increases, the average time delay and its spread around its mean value decrease rapidly, and the reaction proceeds via a more direct mechanism. The comparison between QCT [29] and QM [31] excitation functions for $j = 0$ calculated on the Laganà PES reveals a similar effect. In the QCT case

Table 1
Reaction cross-section (in Å^2) for Li + HF reaction in AP2 PES. The numbers within parentheses indicate the statistical uncertainty in the last significant figure

E_T /meV	$j=0$	$j=1$	$j=2$	$j=3$
20	0.75(2)	0.97(4)	0.86(4)	1.04(5)
40	0.84(3)	1.02(4)	0.81(3)	0.67(4)
64	1.04(2)	1.01(2)	0.76(2)	0.60(2)
88	1.05(2)	0.99(2)	0.68(2)	0.57(2)
130	0.54(1)	0.97(2)	0.58(2)	0.71(2)
157	0.44(1)	1.04(2)	0.54(2)	0.69(2)
190	0.43(1)	1.14(2)	0.56(2)	0.69(2)
239	0.47(1)	1.20(2)	0.52(1)	0.63(2)
280	0.57(2)	1.13(2)	0.51(2)	0.60(2)
320	0.81(2)	0.92(2)	0.48(2)	0.61(2)
377	0.73(2)	0.75(2)	0.46(1)	0.59(1)
416	0.83(2)	0.60(1)	0.44(1)	0.54(1)

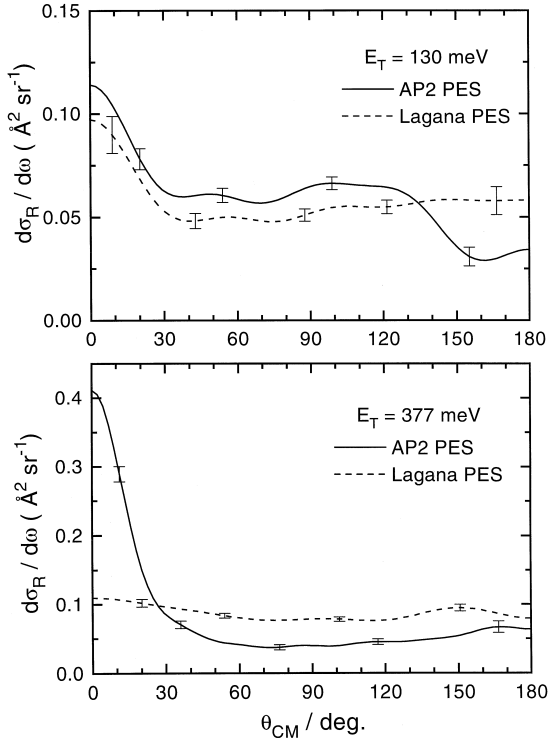

Fig. 2. Comparison of the initial j averaged differential cross-sections (Å^2/sr) for the Li + HF($v = 0, \langle j \rangle$) reaction at 130 (top) and 377 meV (bottom) collision energy calculated on the AP2–PES (solid line) and Laganà PES (dashed line).

[29], the behaviour of the $\sigma_R(E_T)$ resembles that expected for a predominantly attractive PES; it first decays rapidly at collision energies below ≈ 50 meV and then increases smoothly at higher energies yielding ≈ 1 Å^2 at 380 meV. The QM excitation function [31], which was determined in the range from 100 to 400 meV, increases from a low value to 0.9 Å^2 at 250 meV, and then decreases slowly to 0.7 Å^2 at 400 meV. In this PES, the surmounting of the barrier including the zero-point energy of the transition state is endoergic by 32 meV, thus, as in the case of the AP2 PES, one can expect that below 100 meV the product formation will be dominated by tunneling, with a strong resonance structure. At sufficiently high energies, where direct reaction dominates, the QCT and QM $\sigma_R(E_T)$ reach similar values.

The QCT $\sigma_R(E_T)$ on the AP2–PES is also strongly dependent on the initial rotational state, and, as a

result of that, the excitation function averaged over the HF j state distribution of the experiment gives a different behaviour. Table 1 contains the values of the cross-sections at several E_T for initial $j = 0$–3. The $\sigma_R(E_T)$ averaged on the initial distribution of HF rotational states, as well as the absolute values given by Becker et al. (0.8 Å^2 at 130 meV, and 0.94 Å^2 at 377 meV), are shown in the lower panel of Fig. 1. For comparison purposes, the $\sigma_R(E_T)$ averaged on initial j calculated on the Laganà PES is also shown. The excitation function on this PES decays rapidly at low collision energies and then increases smoothly at energies above 125 meV, reproducing somewhat better the experimentally observed tendency. In any case, the results on both PESs are compatible with the experimental cross-sections and, since the uncertainty of the experimental absolute values of the cross-sections is estimated within a factor of two, any conclusion on the accuracy of the PESs or the validity of the QCT method drawn from the comparison with these experimental results must be taken with caution.

Differential cross-sections have been calculated at two of the collision energies where LAB-AD were measured. Fig. 2 shows the comparison between the DCSs average on initial j on AP2 and Laganà PES at collision energies 130 and 377 meV. The averaged DCS on the AP2–PES shows a clear tendency to

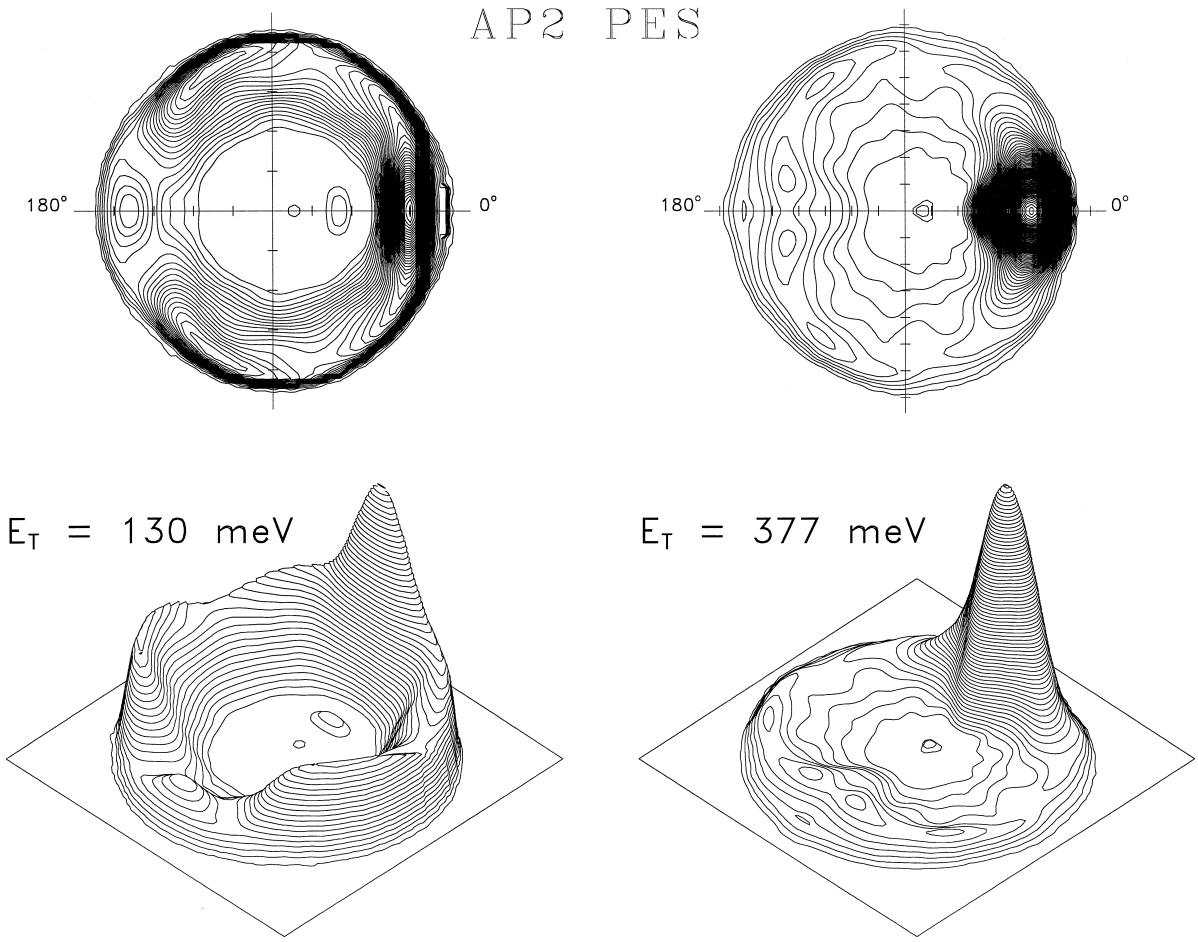

Fig. 3. Three-dimensional perspective and contour polar plots of the triple angle–velocity differential cross-section for the Li + HF → LiF + H reaction at 130 and 377 meV collision energy averaged on initial j, calculated on the AP2–PES. Tick marks represent 50 ms^{-1} in each case.

produce forward scattering, which becomes very prominent at $E_T = 377$ meV. The DCSs calculated on the Laganà PES are more isotropic. At 130 meV, the results on the two PESs are similar, except for the backward scattering. However, at 377 meV, the difference between the DCSs on the two PESs is striking. The DCS on AP2–PES is dominated by the forward peak, whereas that calculated on the Laganà PES is essentially isotropic. It is worth noting that not only the magnitude but also the shape of the DCS is influenced by the rotational state of the HF reagent. On the AP2–PES, at the two collision energies considered here, the forward peak is bigger for initial $j = 1$ (which dominates the experimental j distribution), whereas the DCSs for $j = 0,2,3$ are similar in shape. On the Laganà PES the DCSs for $j = 0–2$ are similar, but for $j = 3$both forward and backward scattering become more prominent at the two collision energies.

The triple angle–velocity DCSs required for the simulation of the LAB ADs were calculated as indicated in Section 2. Figs. 3 and 4 portray the triple angle-velocity DCSs, at 130 and 377 meV, calculated on the AP2 and Laganà PES, respectively. On the AP2–PES the most salient feature is the dominant forward peak, which becomes very sharp at 377 meV. The scattering at 130 meV is more symmetrically distributed in the forward and backward directions than in the case of 377 meV, where the forward scattering is predominant. At the two energies it is

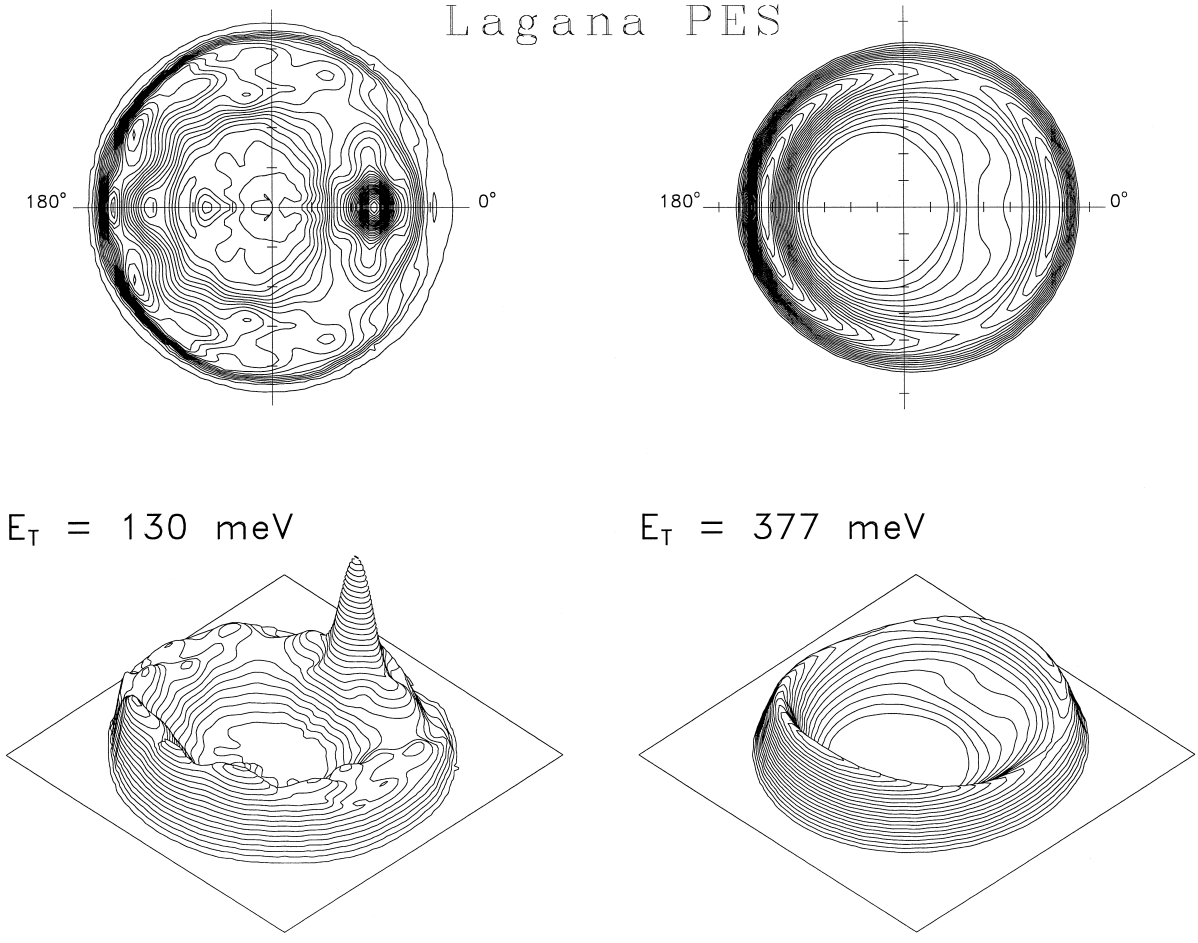

Fig. 4. Same as Fig. 3, but calculated on the Laganà PES.

evident that the translational energy release is quite large and constitutes an important fraction of the total energy available for the products. The angle–velocity polar maps calculated on the Laganà PES are very different. At 130 meV the forward peak dominates, but backward scattering is more important than on the AP2–PES. At 377 meV the polar map is almost totally backward–forward symmetric. In this PES, the recoil velocity distribution is broader than on the AP2–PES.

The angle–velocity coupling is not negligible for this reaction, and the resulting polar maps assuming independent distributions for the two variables are somewhat different. This effect seems to be more marked in the calculation on the Laganà PES. The experimentally deduced polar maps by Becker et al., however, were constructed assuming separable angle and recoil velocity distributions. The comparison between experimental and theoretical polar maps on the AP2–PES renders a qualitative agreement (see figures 13 and 14 of Ref. [1]). The shift from almost symmetric backward–forward to predominantly forward scattering when going from 130 to 377 meV is well accounted for by the present calculations. The results obtained on the Laganà PES are at variance with the experimental results. Whereas at the lowest energy there is a predominance of the forward scattering, at 377 meV the polar map shows no sign of predominance for forward scattering. At this E_T the scattering is essentially isotropic in angles, although the resulting map is not symmetric; the recoil velocity distribution is substantially broader in the forward than in the backward hemisphere.

A better assessment of the capability of the theoretical results to account for the experimental results is obtained by direct simulation of the raw data in the LAB frame. Fig. 5 contains the comparison between the experimental and simulated LAB-ADs at the specified collision energies. The agreement between experimental and simulated LAB-ADs is only qualitative, and it is somewhat better for the results at 377 meV. This comparison reveals that the backward scattering in the theoretical calculations on the AP2–PES is underestimated, at least in relation to the forward scattering. At 130 meV, the experimental data give a maximum at $\approx 75°$, which is not found in the theoretical simulation. The simulations carried out with the triple DCSs calculated on the

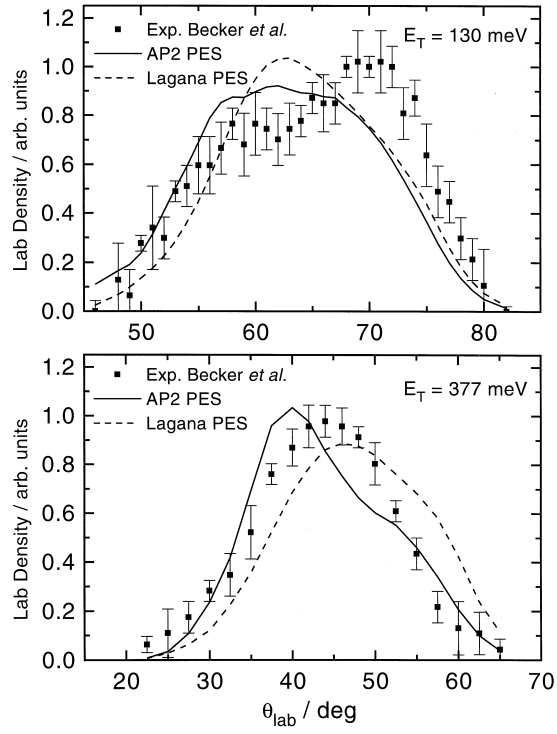

Fig. 5. Experimental (squares) versus simulated LAB-AD for the Li + HF($v = 0$) reaction at the indicated collision energies obtained from calculations on the AP2–PES (solid line) and on the Laganà PES (dashed line).

Laganà PES at 130 and 377 meV are also shown in Fig. 5 (dashed line). On this PES, as shown before (see Figs. 3 and 4), the scattering is more isotropic, and the recoil velocities are smaller. At 377 meV the QCT calculations on this PES predict an excess of backward scattering, but less forward scattering than necessary to match the experimental curve.

In the original paper by Becker et al., based on the nearly symmetric backward–forward behaviour of the DCS at 130 meV, it was argued that the reaction would be essentially coplanar. The present calculations on both PESs yield, however, isotropic DCSs, albeit with a tendency to peak in the forward hemisphere as the collision energy increases in the case of the AP2–PES. Contrary to the arguments of Ref. [1], the analysis of the present calculations indicates that the initial orbital angular momentum, **l**, is broadly distributed with respect to the final relative velocity in a way that the scattering plane, which contains the initial **k** and final **k′** relative velocity

vectors, may form many different angles with that containing **k** and **l**. In addition, for initial $j > 0$, the final orbital angular momentum $\mathbf{l}'$ is broadly distributed around **l**, almost isotropically. This behaviour seems to be the one expected from simple considerations based on statistical models for a $\mathbf{H} + \mathbf{HL} \rightarrow \mathbf{HH} + \mathbf{L}$ reaction, namely $\mathbf{l} \rightarrow \mathbf{j}'$, and $\mathbf{j} \rightarrow \mathbf{l}'$; given an isotropic distribution of initial **j**, this will predict an isotropic distribution of $\mathbf{l}'$. Therefore, there is little basis to conclude that the reaction is dominated by a coplanar mechanism, at least in the range of collision energies investigated here.

The explanation of the differences of the dynamical properties in terms of specific features of the PESs is not simple for this reaction. The minimum of the barrier and its position is similar for the two PESs (182 meV on the Laganà versus 233 meV on the AP2–PES), but the barrier as a function of the Li–F–H bending angle is less steep in the case of the AP2–PES. Furthermore, the collinear Li–F–H barrier is significantly smaller on the latter PES. Nevertheless, the reactivity of the system is larger at low collision energies on the Laganà than on the AP2–PES. On the other hand, as commented on above, the surmounting of the barrier, neglecting the zero-point energy of the saddle point, is an exoergic process on the two PESs and might play a minor role (at least in the QCT calculations) as compared to the features of the PES in the entrance channel, which are different for the two PESs considered in this work.

4. Conclusions

Quasiclassical trajectory (QCT) calculations has been carried out in the range of collision energies and initial rotational quantum numbers relevant to the experiments of Becker et al. The calculations have been performed on the most recent ab initio PES for this system by Aguado et al. (AP2), and the results have been compared with those obtained on a previous partly ab initio PES by Laganà and coworkers, widely used in the literature. Integral and differential cross-sections, as well as the triple angle–velocity differential cross-sections have been determined. On the Laganà PES the differential cross-section averaged on initial HF rotational states becomes more isotropic as the collision energy increases. By contrast, on the AP2 PES forward scattering increases with collision energy, in qualitative agreement with the experimental results. A complete simulation of the experimental laboratory angular distributions have been carried out using the triple differential cross-sections calculated on the two PESs. Only a qualitative agreement between experiment and theory was found.

The effect of initial rotation has been demonstrated to be decisive not only on the integral cross-section and its dependence with the collision energy, but also on the shape of the differential cross-sections.

The comparison of approximate QM results and those obtained in the present work seems to indicate the existence of quantum effects, associated with the zero-point energy of the saddle point, which might be decisive at low collision energies, as is revealed by the comparison of QCT and QM excitation functions calculated on the above-mentioned PESs.

Acknowledgements

We are indebted to M. Paniagua, A. Aguado and O. Roncero for sharing with us their results and for many helpful discussions. This project has been financed by the DGICYT of Spain (PB92-0219-C03). The Scientific Exchange Program 'Acciones Integradas' is also acknowledged.

References

[1] C.H. Becker, P. Casavecchia, P.W. Tiedemann, J.J. Valentini, Y.T. Lee, J. Chem. Phys. 73 (1980) 2833.
[2] H.J. Loesch, S. Stenzel, B. Wüstenbecker, J. Chem. Phys. 95 (1991) 3841.
[3] H.J. Loesch, F. Stienkemeier, J. Chem. Phys. 99 (1993) 9598.
[4] H.J. Loesch, F. Stienkemeier, J. Chem. Phys. 98 (1993) 9570.
[5] G.G. Balint-Kurti, R.N. Yardley, Faraday Discuss. Chem. Soc. 62 (1977) 77.
[6] Y. Zeiri, M. Shapiro, Chem. Phys. 31 (1978) 217.
[7] M. Shapiro, Y. Zeiri, J. Chem. Phys. 70 (1979) 5264.
[8] W.A. Lester Jr., M. Krauss, J. Chem Phys. 52 (1970) 4775.
[9] M.M. Chen, H.F. Schaefer III, J. Chem. Phys. 72 (1980) 4376.
[10] M. Paniagua, A. Aguado, Chem. Phys. 134 (1989) 297.
[11] C. Suárez, A. Aguado, M. Paniagua, Chem. Phys. 178 (1993) 357.

[12] A. Aguado, C. Suárez, M. Paniagua, Chem. Phys. 201 (1995) 107.
[13] S. Carter, J.N. Murrell, Mol. Phys. 41 (1980) 567.
[14] E. García, A. Laganá, Mol. Phys. 52 (1984) 1115.
[15] P. Palmieri, A. Laganà, J. Chem. Phys. 91 (1989) 7302.
[16] G.A. Parker, A. Laganà, S. Crocchianti, R.T. Pack, J. Chem. Phys. 102 (1995) 1238.
[17] A. Aguado, M. Paniagua, M. Lara, O. Roncero, J. Chem. Phys. 106 (1997) 1013.
[18] R.B. Walker, Y. Zeiri, M. Shapiro, M.J. Chem. Phys. 74 (1981) 1763.
[19] J.M. Alvariño, P. Casavecchia, O. Gervasi, A. Laganà, J. Chem. Phys. 77 (1982) 6341.
[20] I. Noorbatcha, N. Sathyamurthy, Chem. Phys. 77 (1983) 67.
[21] J.M. Alvariño, M.L. Hernández, E. García, A. Laganà, J. Chem. Phys. 84 (1986) 3059.
[22] A. Laganà, E. García, Chem. Phys. Lett. 139 (1987) 140.
[23] A. Laganà, O. Gervasi, E. García, Chem. Phys. Lett. 143 (1988) 174.
[24] A. Laganà, E. García, O. Gervasi, J. Chem. Phys. 89 (1988) 7238.
[25] A. Laganà, X. Giménez, E. García, O. Gervasi, Chem. Phys. Lett. 176 (1991) 280.
[26] G.G. Balint-Kurti, F. Gögtas, S.P. Mort, A.R. Offer, A. Laganà, O. Gervasi, J. Chem. Phys. 99 (1993) 9567.
[27] M. Baer, H.J. Loesch, H.J. Werner, I. Last, Chem. Phys. Lett. 219 (1994) 372.
[28] M. Baer, I. Last, H.J. Loesch, J. Chem. Phys. 101 (1994) 9648.
[29] A. Laganà, G. Ochoa de Aspuru, A. Aguilar, X. Giménez, J.M. Lucas, J. Phys. Chem. 99 (1995) 11696.
[30] F. Gögtas, G.G. Balint-Kurti, A.R. Offer, J. Chem. Phys. 104 (1996) 7927.
[31] W. Zhu, D. Wang, J.Z.H. Zhang, Theor. Chem. Acc. 96 (1997) 31.
[32] A. Aguado, M. Paniagua, M. Lara, O. Roncero, J. Chem. Phys. 107 (1997) 10085.
[33] F.J. Aoiz, V.J. Herrero, V. Sáez Rábanos, J. Chem. Phys. 97 (1992) 7423.
[34] F.J. Aoiz, L. Bañares, T. Díez-Rojo, V.J. Herrero, V. Sáez Rábanos, J. Phys. Chem. 100 (1996) 4071.
[35] M. Brinkhoff, Diplomarbeit, Universität Bielefeld (1986).